Supplementary Information (SI) for Lab on a Chip.

Supporting information

A Microfluidic Platform for studying Supercritical fluid crystallization and its Applications

Fatma Ercicek[a,b], Arnaud Erriguible[a], Olivier Nguyen[a], Christelle Harscoat-Schiavo[b], Pascale Subra-Paternault[b], Samuel Marre[a*]

Section 1. Materials and methods

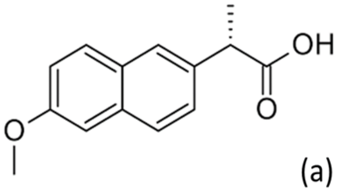

(a)

(b)

Figure S1: Structures of (a) S-Naproxen and (b) 4,4’-Bipyridine.

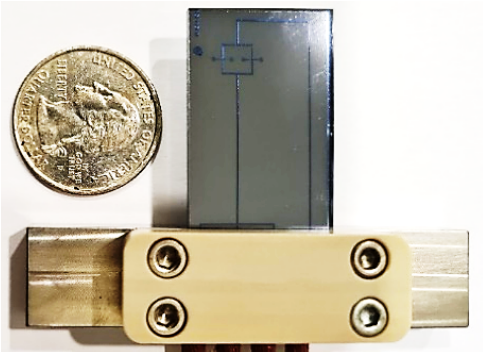

Figure S2: Picture of the microreactor developed and used in this study, packed inside its compression part allowing connecting it to external fluidic equipment.

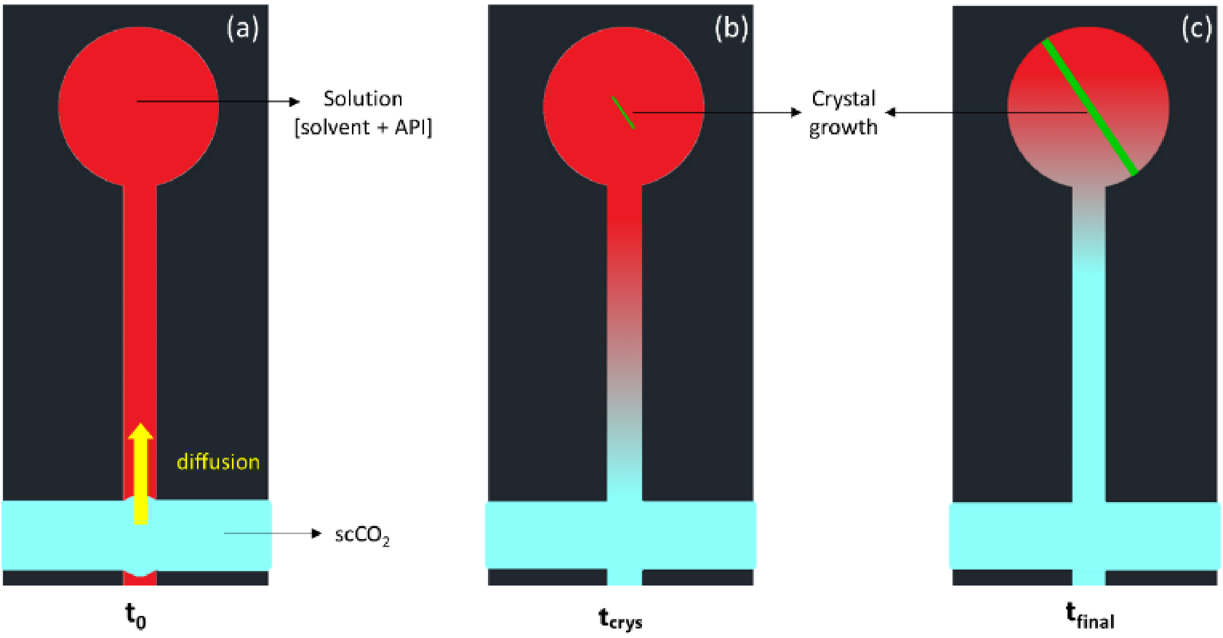

Figure S3: Scheme of the diffusion-driven anti-solvent crystallization step: (a) CO_2 addition, time = 0 s, (b) first detection of a crystal, time = crystal detection time (t_{crys}), and (c) final habitat of the crystal after growth.

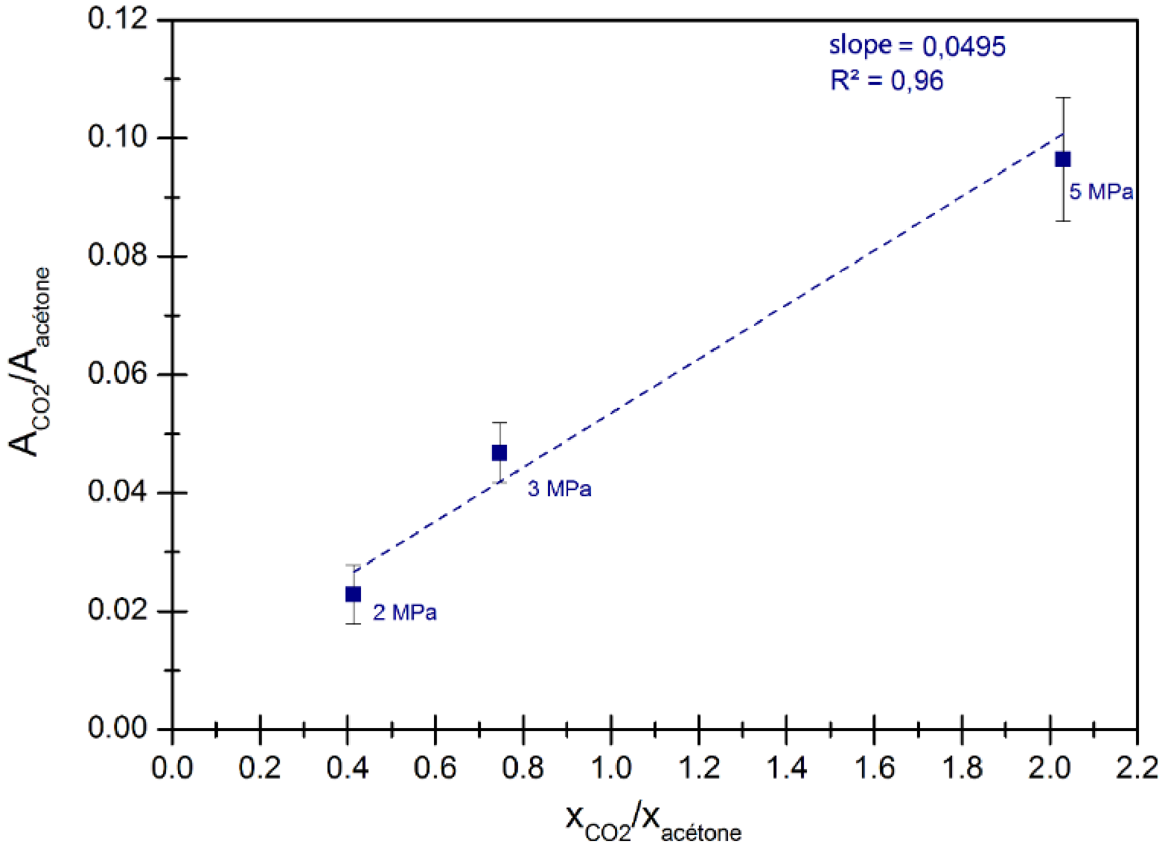

Figure S4: Calibration curve for quantitative analysis by Raman spectrometry at 40°C, the slope value is 0.0495 with a $R^2=0.95$.

Section 2. Numerical modelling

The Navier-Stokes equations are solved for an incompressible single-phase flow formulation assuming negligible gravity forces. It reads:

$$\nabla . u = 0$$

$$\rho\left(\frac{\partial u}{\partial t} + u . \nabla u\right) = - \nabla p + \nabla . \left(\mu\left(\nabla u + \nabla^T u\right)\right)$$

in which p is the pressure, ρ the density of the fluid, μ the dynamic viscosity, t the time and **u** the velocity vector.

The Peng Robinson equation of state (PR-EOS) with quadratic mixing rules is used for calculating the density of the fluid:

$$P = \frac{N\,R\,T}{V - N\,b_m} - \frac{a_m\,N^2}{\left(V - N\,b_m\,m_1\right)\left(V - N\,b_m\,m_2\right)}\#$$

$$m_1 = - 1 + \sqrt{2}\#$$

$$m_2 = - 1 - \sqrt{2}\#$$

For each compound i:

$$a_i = 0.45724\,\frac{R^2\,T_{c,i}^2}{P_{c,i}}\#$$

$$b_i = 0.07780\,\frac{R\,T_{c,i}}{P_{c,i}}\#$$

$$\alpha_i = \left[1 + \kappa_i\left(1 - T_{r,i}^{0.5}\right)\right]^2\#$$

$$T_{r,i} = \frac{T}{T_{c,i}}\#$$

$$\kappa_i = \left(0.37464 + 1.54226\,\omega_i - 0.26992\,\omega_i^2\right)\#$$

The Van der Walls mixing rule is chosen for its ease of application and relatively good accuracy:

$$a_m = \sum_i \sum_j x_i\,x_j\,(a\alpha)_{ij}\#$$

$$b_m = \sum_i x_i\,b_i\#$$

$(a\alpha)_{ij} = (1 - k_{ij})\sqrt{(a_i\,\alpha_i)\,(a_j\,\alpha_j)}\#$

$k_{ij} = k_{ji}\#$

$k_{ii} = 0\#$

with k_{ij} the binary interaction parameters.

The species continuity equation of the acetone (1: acetone, 2: CO2) is expressed by considering advection and non-ideal diffusion :

$$\frac{\partial \rho \omega_1}{\partial t} + \nabla \cdot (\rho \omega_1 u) - \rho D_{12}(1 + C^{nonideal})\nabla \omega_1 = 0$$

$$C^{nonideal} = x_1\left(\frac{\partial ln(\varphi_1)}{\partial x_1} - \frac{\partial ln(\varphi_1)}{\partial x_2}\right)$$

$$\sum_i \omega_i = 1 \qquad \text{for i=1,2}$$

with ω_1 and x_1 the mass fraction and the molar fraction of the solvent respectively.

D_{12} is the diffusion of solvent/CO_2 system calculated by the Hayduck-Minhas relation:

$$D_{12} = 13.3 \times 10^{-8} V_1^{-0.71} \mu_2^{\left(\frac{10.2}{V_1} - 0.791\right)} T^{1.47}$$

where V_1 is the molar volume of pure acetone calculated by the Peng Robinson equation of state and m_2 the viscosity of pure CO2.

According to the Peng Robinson equation of state, the fugacity is computed by:

$$ln(\varphi_i) = \frac{b_i}{b_m}(Z - 1) - ln(Z - B) - \frac{A}{2\sqrt{2}\,B}\left(\frac{2}{a_m}\sum_j x_j\,(a\alpha)_{ij} - \frac{b_i}{b_m}\right) ln\left[\frac{Z + (1 + \sqrt{2})\,B}{Z + (1 - \sqrt{2})\,B}\right]\#$$

and its derivative by:

$$\left(\frac{\partial ln(\varphi_i)}{\partial x_j}\right)_{T,P} = - \frac{(\partial V/\partial x_j) - b_j}{V - b_m} - \frac{b_i b_j}{b_m^2}(Z - 1) + \frac{b_i Z\,\partial V}{b_m V \partial x_j} - \frac{a_m(b_j V - b_m(\partial V/\partial x_j))((1/a_m)(\partial a_m/\partial x}{RTb_m V} {}_*$$

$$\frac{1}{2\sqrt{2}RTb_m}\left[\frac{\partial^2 a_m}{\partial x_i \partial x_j} - \frac{b_j\,\partial a_m}{b_m\,\partial x_i} - \frac{b_i\,\partial a_m}{b_m\,\partial x_j} + \frac{2a_m b_i b_j}{b_m^2}\right] ln\left[\frac{V + (1 + \sqrt{2})b_m}{V + (1 - \sqrt{2})b_m}\right]$$

$$\frac{\partial a_m}{\partial x_i} = 2\sum_j x_j(1 - k_{ij})\sqrt{a_i a_j}$$

$$\frac{\partial^2 a_m}{\partial x_i \partial x_j} = 2(1 - k_{ij})\sqrt{a_i a_j}$$

$$V_* = V^2 + 2b_m V - b_m^2$$

$$\frac{\partial V}{\partial x_i} = \frac{V_*\left(\partial a_m/\partial x_i\right) - \left[2a_m(V - b_m) + RTV_*^2/(V - b_m)^2\right]b_i}{2a_m(V + b_m) - RTV_*^2/(V - b_m)^2}$$

Numerical methods

The partial differential system is solved numerically by the in-house Fortran massively parallel CFD code [1], developed at the Institute of Mechanical Engineering (I2M-TREFLE). Notus is an open source software based on the finite volume method. The Navier-Stokes equation is solved in two steps by the time-splitting algorithm of Goda [2]. The advection term is discretized by the second order scheme in space (total variation diminishing with superbee flux limiter function (TVD superbee)) [3] and an implicit second order central discretization is applied in space for the diffusion term. The variable fields are solved, with an iterative solver (Hypre Bicg-Stab solver), on a fixed velocity/pressure staggered grid by ensuring the time and space convergence.

[1] Notus computational fluid dynamics, v0.6.0. [https://notus-cfd.org/], 2024.

[2] Goda, K., 1979. A multistep technique with implicit difference schemes for calculating two- or three-dimensional cavity flows. Journal of Computational Physics 30, 76–95.

[3] Roe, P.L., 1986. Characteristic-Based Schemes for the Euler Equations. Annual Review of Fluid Mechanics 18, 337–365.

Section 3. CO_2-acetone thermodynamics

On the binary diagram of the CO_2-acetone mixture, for any pressure where both phases are present (biphasic domain), a certain amount of CO_2 in the liquid phase is in equilibrium with a certain amount of CO_2 in the vapor phase. These mole fractions correspond to the points where the isobar crosses the dew and bubble curves, respectively. A plot at 6 MPa has been drawn as an example in Figure S1.a. The CO_2-acetone mixture shows a wide range where both phases coexist, underlining the good miscibility of these two compounds. The critical point of this mixture is at 8 MPa, so that above this pressure, the mixture becomes single-phase supercritical.

The CO_2-acetone vapor-liquid equilibrium (VLE) at 40°C and the theoretical composition of CO_2 versus acetone in the microreactor are represented in Figure S1.b.

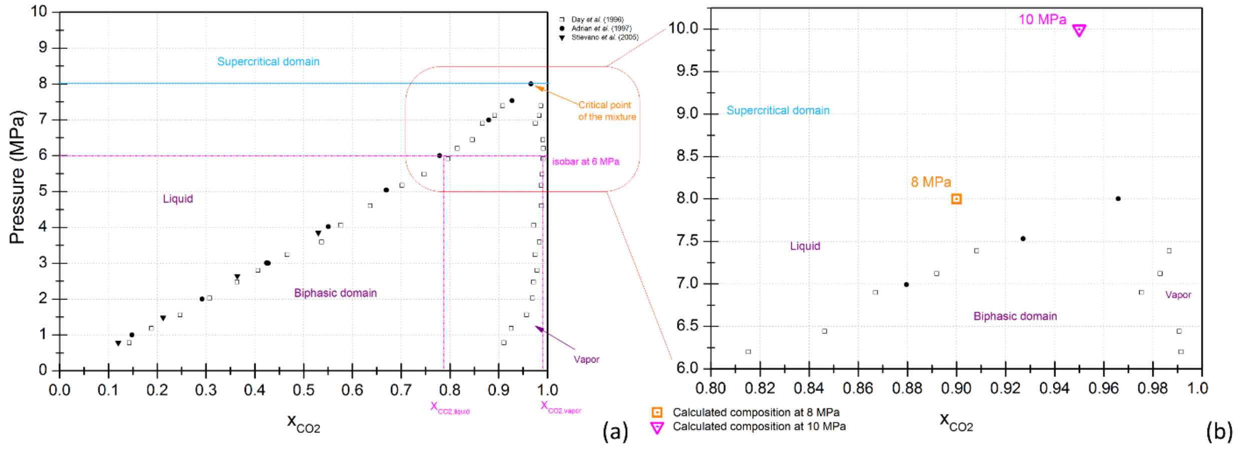

Figure S5: (a) CO_2-acetone vapor-liquid equilibrium at 40°C and (b) the theoretical composition in the microreactor regarding the VLE.

Section 4. Crystal growth and kinetics as a function of C_0

- **$C_0 = 20$ mg.mL^{-1}**

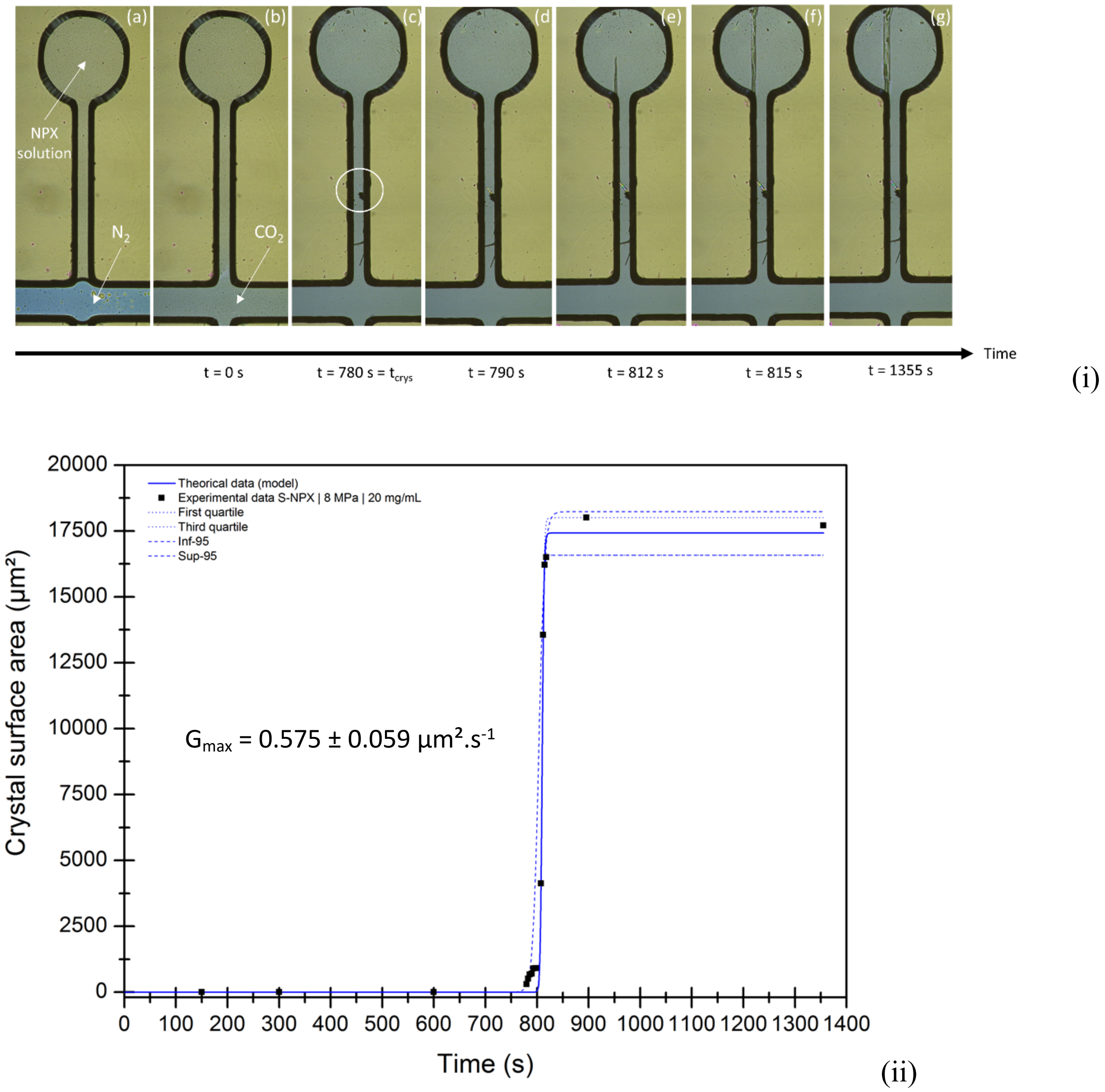

Figure S6: (i) Experimental images acquired during S-NPX precipitation with $scCO_2$ at 20 mg/mL under 8 MPa: (a) N_2 flush, (b) CO_2 introduction, (c) first apparition of NPX crystals, (d), (e) and (f) crystal growth, and (g) the final crystal habit. (ii) Example of the logistic model (solid line) fitting the growth data (black squares) of S-NPX at 20 mg/mL under 8 MPa. Dotted lines - - - represent the 5 and 95% confidence intervals, while the · · · are the first and third quartiles.

- **$C_0 = 40$ mg.mL^{-1}**

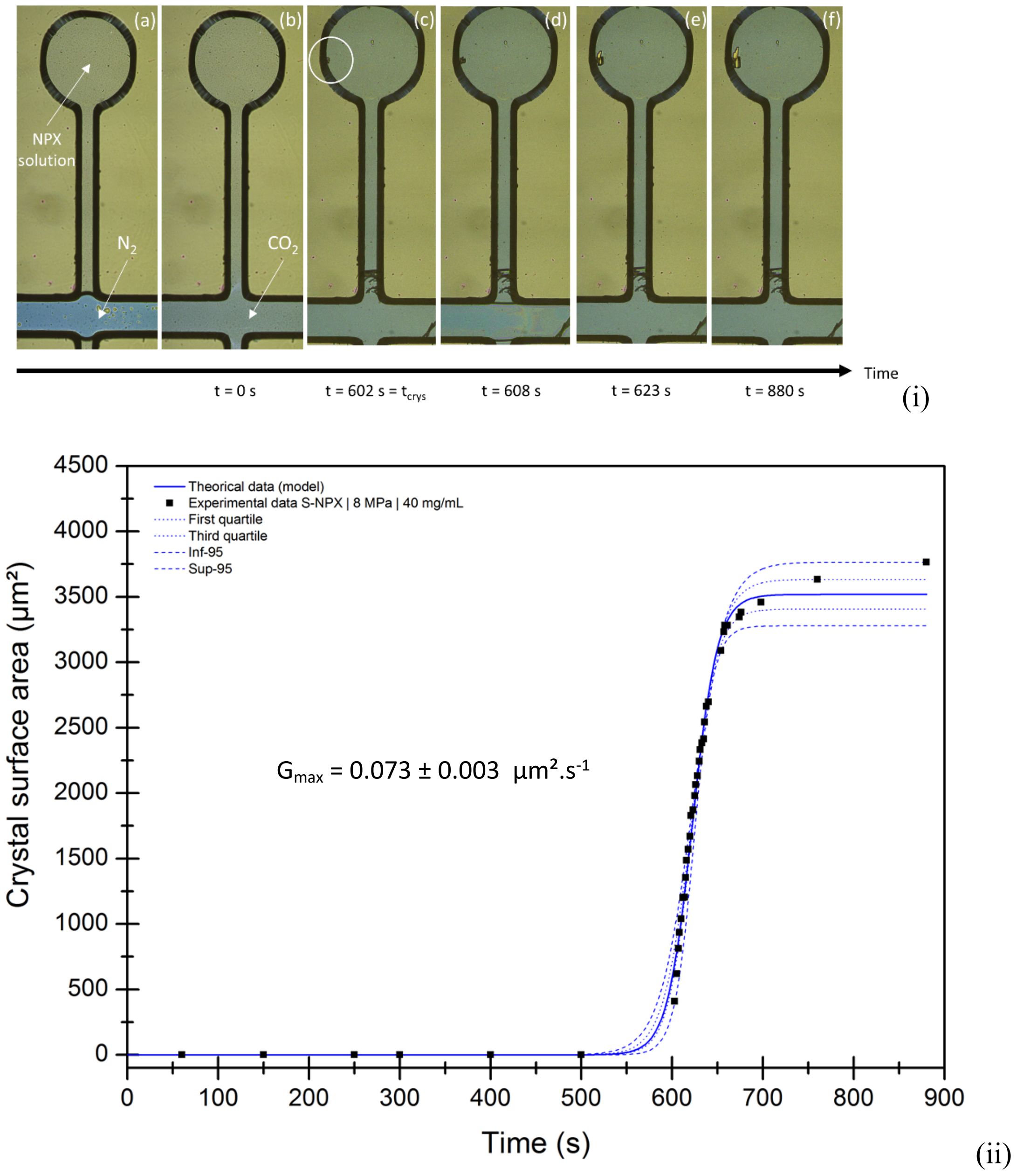

Figure S7: (i) Experimental images acquired during S-NPX precipitation with $scCO_2$ at 40 mg/mL under 8 MPa: (a) N_2 flush, (b) CO_2 introduction, (c) first apparition of NPX crystals, (d), (e) crystal growth (in a cubic shape), and (f) the final crystal habit. (ii) Example of the logistic model (solid line) fitting the growth data (black squares) of S-NPX at 40 mg/mL under 8 MPa. Dotted lines - - - represent the 5 and 95% confidence intervals, while the · · · are the first and third quartiles.

- **C_0 = 100 mg.mL^{-1}**

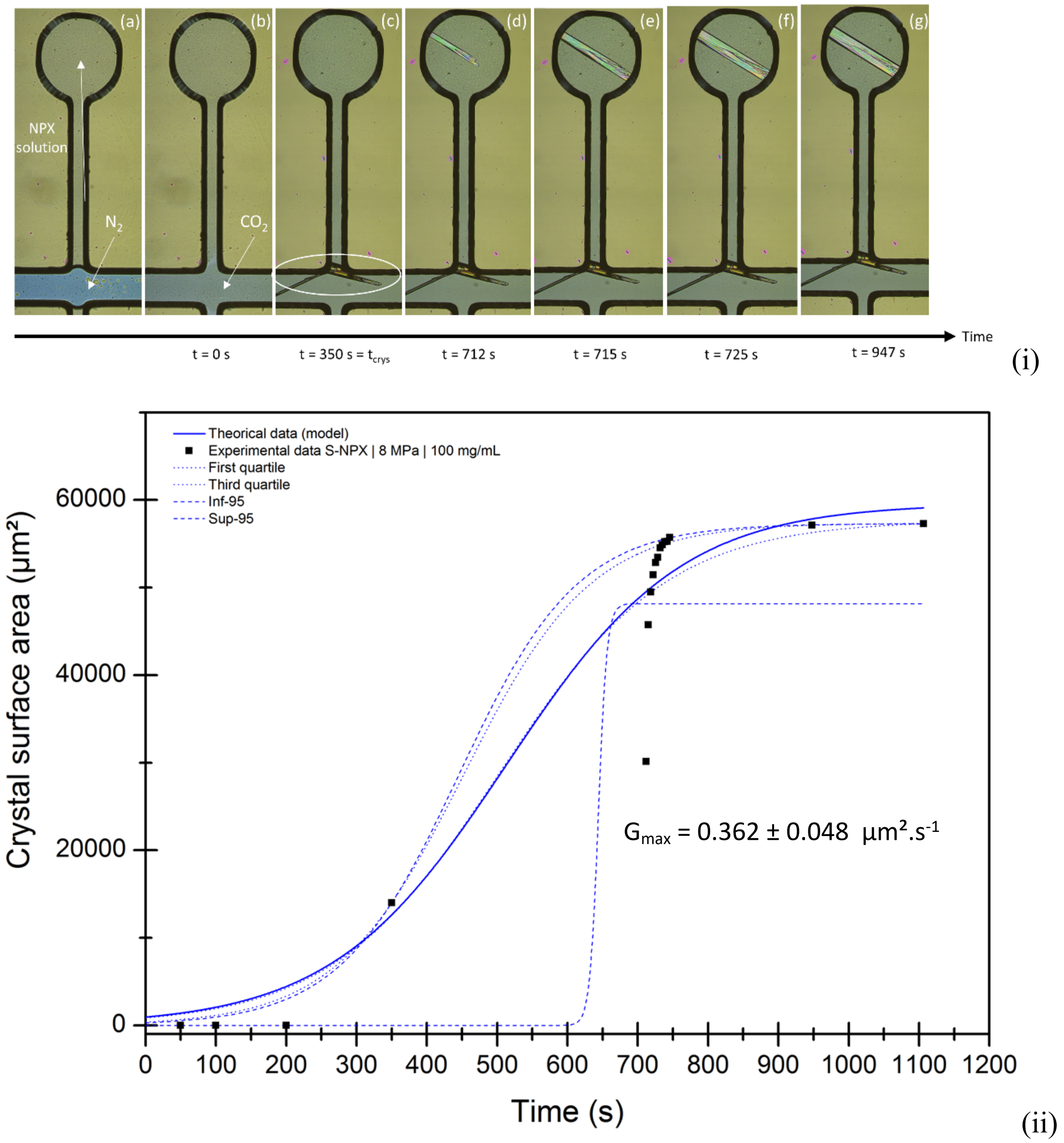

Figure S8: (i) Experimental images acquired during S-NPX precipitation with $scCO_2$ at 100 mg/mL under 8 MPa: (a) N_2 flush, (b) CO_2 introduction, (c) first apparition of NPX crystals, (d), (e) and (f) crystal growth, and (g) the final crystal habit. (ii) Example of the logistic model (solid line) fitting the growth data (black squares) of S-NPX at 100 mg/mL under 8 MPa. Dotted lines - - - represent the 5 and 95% confidence intervals, while the · · · are the first and third quartiles.